(3) MacKnight, W. J.; Earnest, T. R., Jr. *J. Polym. Sci., Macromol. Rev.* **1981**, *16*, 41.
(4) MacKnight, W. J.; Taggart, W. P.; Stein, R. S. *J. Polym. Sci., Polym. Symp.* **1974**, *No. 45*, 113.
(5) Eisenberg, A. *Macromolecules* **1970**, *3*, 147.
(6) Wilson, F. C.; Longworth, R.; Vaughan, D. J. *Polym. Prepr., Am. Chem. Soc., Div. Polym. Chem.* **1968**, *9*, 505.
(7) Gierke, T. D.; Munn, G. E.; Wilson, F. C. *J. Polym. Sci., Polym. Phys. Ed.* **1981**, *19*, 1687.
(8) Marx, B. C. L.; Caulfield, D. F.; Cooper, S. L. *Macromolecules* **1973**, *6*, 344.
(9) Roche, E. J.; Stein, R. S.; MacKnight, W. J. *J. Polym. Sci., Polym. Phys. Ed.* **1980**, *10*, 1035.
(10) Roche, E. J.; Stein, R. S.; Russell, T. P.; MacKnight, W. J. *J. Polym. Sci., Polym. Phys. Ed.* **1980**, *18*, 1497.
(11) Rahrig, D. B. Ph.D. Thesis, University of Massachusetts, 1978.
(12) Rahrig, D.; MacKnight, W. J. *Adv. Chem. Ser.* **1980**, *No. 187*, 91.
(13) Sanui, K.; MacKnight, W. J.; Lenz, R. W. *J. Polym. Sci., Part B* **1973**, *11*, 427.
(14) Ihel, K. *J. Appl. Crystallogr.* **1976**, *9*, 296.
(15) Conway, B. E. "Ionic Hydration in Chemistry and Biophysics"; Elsevier: New York, 1981.
(16) Roche, E. J.; Pineri, M.; Duplessix, R.; Levelut, A. M. *J. Polym. Sci., Polym. Phys. Ed.* **1981**, *19*, 1.
(17) Mauritz, K. A.; Lowry, S. R. *Polym. Prepr., Am. Chem. Soc., Div. Polym. Chem.* **1978**, *19* (2), 336.
(18) Komoroski, R. A. *Adv. Chem. Ser.* **1980**, *No. 187*, 156.
(19) Guinier, A.; Fournet, G. "Small Angle Scattering of X-Rays"; Wiley: New York, 1955.

Small-Angle Neutron Scattering from Elastomeric Networks. Application to Labeled Chains Containing Several Cross-Links†

Robert Ullman

Engineering and Research Staff, Ford Motor Company, Dearborn, Michigan 48121.
Received February 23, 1982

ABSTRACT: The scattering law for polymer chains in rubber networks has been calculated for the case where the labeled chains contain multiple cross-links. Emphasis is placed on changes in molecular dimensions induced by stretching or swelling. The results differ appreciably from the scattering of end-linked chains in polymer networks in two important ways. First, the chains with multiple cross-links exhibit the anisotropy of macroscopic deformation to a greater extent than end-linked chains. Second, junction fluctuations have a profound influence on chain shape in end-linked chains and are of much less importance in the multilinked case. Since anisotropy in chain deformation is higher in multilinked labeled chains that deform affinely in the mean coordinates, it is relatively easy to determine whether the affine model is valid in real materials. Comparison of the calculation with the one published experiment indicates that deformation on the molecular scale is less than would be expected.

I. Introduction

The molecular dimensions of polymer molecules in bulk can be determined by small-angle neutron scattering (SANS).[1,2] This is achieved by replacing some of the polymer by deuterium-labeled chains.

The SANS method has been exploited in following the changes in molecular dimensions upon stretching or swelling of elastomers as well.[3-8] All these experiments except those of Clough et al.[5] were performed with networks composed of end-linked polymer molecules, and the theory of SANS for rubbers has been developed for these materials.[9-11]

As model rubbers, the end-linked networks are, in principle, more easily characterized and because chain lengths may be kept uniform, more regular in their structure. In general, they are more troublesome to prepare than randomly cross-linked networks. Incomplete cross-linking changes the elastic properties of a network substantially and can lead to incorrect interpretation of otherwise carefully performed experiments. The errors thus induced are greater for end-linked networks and also more serious if the network is trifunctional.

Networks constructed with multiple cross-links on a labeled chain tend to be irregular with variable distances between cross-links and variable numbers of cross-link junctions per chain. The influence of defects is not serious if the number of cross-links per original polymer molecule is sufficiently large.

† Work supported in part by National Science Foundation Grant No. DMR-79-26254.

Deuterated polymer chains incorporated in a network by end-linking are randomly arranged, and therefore the scattering from such an assembly is the sum of the contributions from each molecule, with no contribution from interactions between different molecules. Labeled polymer molecules incorporated into a network with multiple cross-links are also randomly arranged, but the various submolecules between cross-links originating from the same prepolymer molecule are coherently arranged, and contributions from pairs of monomer units on different submolecules must be included in the scattering formulas.

As will be seen, the scattering from multiply-linked elastomers is very different from that of end-linked elastomers, and this difference can be extremely useful in assessing the reliability of models of rubber elasticity.

II. Scattering Theory for Multiply-Linked Elastomers

The excess coherent elastic neutron scattering from D-labeled polymer chains in an H matrix is given by

$$I(\mathbf{q}) = A(b_D - b_H)^2 McS(\mathbf{q}) \quad (1)$$

In this equation, $I(\mathbf{q})$ is the scattering intensity at a wave vector $\mathbf{q}$, $\mathbf{q} = (2\pi/\lambda)(\mathbf{k} - \mathbf{k}_0)$ (where $\mathbf{k}_0$ and $\mathbf{k}$ are unit vectors in the directions of incident and scattered rays), λ is the wavelength of the neutrons, and the magnitude of $\mathbf{q}$ equals $(4\pi/\lambda) \sin(\theta/2)$ (where θ is the angle between $\mathbf{k}_0$ and $\mathbf{k}$). A is a lumped constant containing machine parameters and some physical constants, b_H and b_D are scattering lengths of H and D monomer units, M is the molecular weight of the polymer, and c is the concentration in grams per milliliter. $S(\mathbf{q})$, the scattering law or particle

0024-9297/82/2215-1395$01.25/0

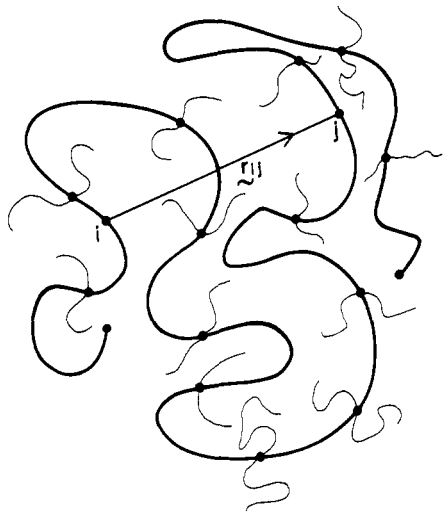

Figure 1. Schematic diagram of a multiply-cross-linked polymer chain in a polymer network. The vector $\mathbf{r}_{ij}$ connects monomer unit i, which is in the second submolecule, to monomer unit j, which is in the tenth submolecule.

scattering factor, is a representation of the ensemble average shape and size of the labeled molecules in the network. It is given by

$$S(\mathbf{q}) = \frac{1}{N^2}\sum_{i,j}\langle\exp(i\mathbf{q}\cdot\mathbf{r}_{ij})\rangle \tag{2}$$

The quantity $\mathbf{r}_{ij}$ is the vector connecting monomer i to monomer j. There are N monomer units in a polymer molecule, and the sum is carried out over all units i and j in a single polymer molecule. The labeled molecules are taken to be randomly arranged, and there is no contribution to the coherent scattering from monomer units on different chains.

Consider a polymer molecule cross-linked at k points. The chain is divided into $k + 1$ submolecules, two of which are dangling ends that do not deform as the network is stretched. To simplify the calculation, we take all submolecules to be of equal length, each containing n monomers, from which it follows that $n(k + 1) = N$. Figure 1 is a schematic model of such a chain. It is to be noted that i and j can have several relative arrangements in the network, and the contribution to the scattering of each pair will depend on these arrangements. The cross-link points are pinned to the network, and these are presumed to move with the macroscopic deformation of the material. The distribution of monomers in space is governed by Gaussian statistics subject to the constraints imposed on the cross-link junctions. Table I contains a classification of the various ways segments i and j are distributed on the polymer molecule and the multiplicity of each arrangement. In working through the calculations of $S(\mathbf{q})$, one must treat the different cases separately. It is evident from the multiplicity that term E becomes dominant as k becomes large.

Regardless of the constraints on the molecule, the probability that monomer units i and j are separated by $\mathbf{r}_{ij}$ is of the form $A\exp(-a_1x_{ij}^2 - a_2y_{ij}^2 - a_3z_{ij}^2)$, a_1, a_2, and a_3 differing when the system is anisotropically deformed. Accordingly, $S(\mathbf{q})$ may be written

$$S(\mathbf{q}) = \frac{1}{N^2}\sum_{i,j}\exp\left[-\frac{1}{2}(q_x^2\langle x_{ij}^2\rangle + q_y^2\langle y_{ij}^2\rangle + q_z^2\langle z_{ij}^2\rangle)\right] \tag{3}$$

The task of calculation is considerably simplified since the scattering law is completely determined by the mean square distance between pairs of monomer units.

Table I
Arrangements of Monomer Units i and j on Submolecules of a Labeled Network Chain

case	type	multiplicity
A	i and j are both on the same end submolecule	2
B	i and j are on different end submolecules	2
C	one unit is on an end submolecule and the other on an internal submolecule	$4(k - 1)$
D	i and j are on the same internal submolecule	$k - 1$
E	i and j are on different internal submolecules	$(k - 1)(k - 2)$

The calculation of $S(\mathbf{q})$ in the general anisotropic case is most easily followed by consideration of one of the Cartesian components. The results depend on the relationship between the macroscopic deformation and molecular deformation. For this purpose, we have based the analysis on the phantom network model, noting that several variants of that model may be encompassed within the analysis with only minor modifications of the calculation. The phantom network is characterized as follows:

1. The network deforms affinely so that the macroscopic deformation of the sample and the deformation of the mean vectors connecting cross-link points are the same. Monomer units between cross-link points are free to move consistent with constraints imposed at the cross-links.

2. Neither the volume occupied by monomer units nor the blocking of one chain's deformation by the material presence of other chains is directly taken into account in calculation of chain statistics or chain deformation.

3. Submolecules with the same number of monomer units have very different mean end-to-end distances. This arises because of topological constraints and because of the volume displaced by other parts of the network. The distribution of mean end-to-end distances in the ensemble is Gaussian.

4. The junction points fluctuate in position owing to Brownian motion. In the phantom network model, these fluctuations are calculable and large, depend strongly on network functionality, are isotropic, and are independent of sample deformation and the mean distance between chain ends. Using an overbar to designate a time average and angular brackets to designate an ensemble average, we have

$$Z = \bar{Z} + \delta Z \tag{4a}$$

$$\langle Z^2\rangle = \langle\bar{Z}^2\rangle + \langle(\delta Z)^2\rangle \tag{5}$$

where Z is the z component of the vector connecting the ends of a submolecule and δZ is the instantaneous fluctuation from a mean position. It follows from eq 5 and the independence of $\langle(\delta Z)^2\rangle$ on deformation that $\langle Z^2\rangle$ does not deform affinely.

Consider next the mean square moments for each of the cases listed in Table I. The reduced variables u, v, and w are introduced to simplify the equations. If the monomer units are numbered from 1 to N, u equals the fraction of monomers to the left of i in the same submolecule. In particular, if i is on the pth submolecule (out of $k + 1$), $u = i/n - p$. Similarly, $v = j/n - p$, and w, which is only used if i and j are on the same submolecule, $= |i - j|/n$. The cross-link points are labeled with the vector coordinates $\mathbf{R}_1$, $\mathbf{R}_2$, ..., $\mathbf{R}_k$ and the Cartesian coordinates of $\mathbf{R}_p$ are (X_p, Y_p, Z_p). The shorthand notation $\mathbf{R}_{12} = \mathbf{R}_2 - \mathbf{R}_1$ and $\mathbf{R}_{pq} = \mathbf{R}_q = \mathbf{R}_p$ is used. The Cartesian components are similarly labeled.

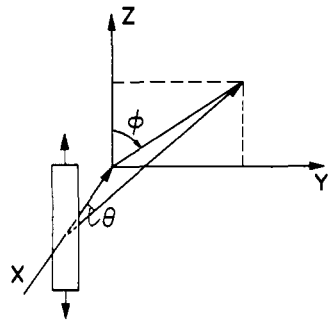

Figure 2. Diagram of a uniaxially stretched polymer sample in the geometry of a neutron scattering spectrometer.

In case A, the monomer units are unaffected by network deformation

$$\langle z_{ij}^2 \rangle = nb^2w/3 \tag{6}$$

b is the length of a monomer unit. Case B differs in that the separation of segments is influenced by sample deformation. Thus

$$\langle z_{ij}^2 \rangle = \frac{nb^2}{3}(1 - u + v) + \langle Z_{1k}^2 \rangle \tag{7}$$

For case C, $\langle z_{ij}^2 \rangle$ is obtained by summing three terms, the distance from segment i to the first cross-link, the distance from the first cross-link to the pth cross-link, and the distance between the pth cross-link and monomer j. The result is

$$\langle z_{ij}^2 \rangle = (nb^2/3)(1 - u) + \langle Z_{1p}^2 \rangle + (nb^2/3)v(1 - v) + v^2\langle Z_{p,p+1}^2 \rangle \tag{8}$$

Case D is identical with that for end-linked chains.[11]

$$\langle z_{ij}^2 \rangle = (nb^2/3)w(1 - w) + w^2\langle Z_{12}^2 \rangle \tag{9}$$

Case E is calculated for monomer i lying between cross-link p and $p + 1$ and monomer j lying between cross-links q and $q + 1$, q taken for convenience as greater than p.

$$\langle z_{ij}^2 \rangle = (nb^2/3)u(1 - u) + u^2\langle Z_{p,p+1}^2 \rangle + (nb^2/3)v(1 - v) + v^2\langle Z_{q,q+1}^2 \rangle + \langle Z_{p+1,q}^2 \rangle \tag{10}$$

The summations in eq 3 are converted to integrals according to

$$\sum_{i,j=1}^{N}(\ ) = \sum_{\mathrm{A}}^{\mathrm{E}}\int_0^n\int_0^n(\ )\,di\,dj = n^2\sum_{\mathrm{A}}^{\mathrm{E}}\int_0^1\int_0^1(\ )\,du\,dv = 2n^2\sum_{\mathrm{A}}^{\mathrm{E}}\int_0^1(\ )(1 - w)\,dw \tag{11}$$

The symbol $\sum_{\mathrm{A}}^{\mathrm{E}}$ refers to a sum taken over all categories of pairs i and j.

To establish a frame of reference for the scattering experiment, we define a coordinate system. A picture of the arrangement is presented in Figure 2. The neutron beam impinges on the sample in the negative X direction, and the detector lies in the YZ plane. Since scattering is at a small angle, $q_x \approx 0$, $q_y = q \sin\phi$, and $q_z = q \cos\phi$, where ϕ is the azimuthal angle measured clockwise from the Z axis. $S(\mathbf{q})$ becomes

$$S(\mathbf{q}) = \frac{n^2}{N^2}\sum_{\mathrm{A}}^{\mathrm{E}}\int\int\exp\left[-\frac{1}{2}q^2(\langle z_{ij}^2 \rangle \cos^2\phi + \langle y_{ij}^2 \rangle \sin^2\phi)\right] du\,dv \tag{12}$$

If the system is deformed isotropically, $\langle y_{ij}^2 \rangle = \langle z_{ij}^2 \rangle = \langle r_{ij}^2 \rangle/3$ and eq 12 reduces to

$$S(\mathbf{q}) = \frac{n^2}{N^2}\sum_{\mathrm{A}}^{\mathrm{E}}\int\int\exp\left[-\frac{1}{6}q^2\langle r_{ij}^2 \rangle\right] du\,dv \tag{13}$$

It is convenient to examine the scattering along the principal axes of sample deformation. If these are set parallel to the Y and Z axes, we find

$$S_{\parallel}(\mathbf{q}) = \frac{n^2}{N^2}\sum_{\mathrm{A}}^{\mathrm{E}}\int\int\exp\left[-\frac{1}{2}q^2\langle z_{ij}^2 \rangle\right] du\,dv \tag{14a}$$

$$S_{\perp}(\mathbf{q}) = \frac{n^2}{N^2}\sum_{\mathrm{A}}^{\mathrm{E}}\int\int\exp\left[-\frac{1}{2}q^2\langle y_{ij}^2 \rangle\right] du\,dv \tag{14b}$$

The z component is taken as the parallel direction and y as perpendicular to correspond to the common uniaxial deformation case. If deformation is biaxial, the SANS spectrum must be collected at two different sample orientations in order to completely specify the chain deformation.

The wave vector and unperturbed chain dimensions appear in the scattering law as a single combined variable $x = nb^2q^2/6$. Henceforth, $S(\mathbf{q})$ will be written as $S(x)$ in the text. The separate parts of $S(x)$ are as follows:

$$S_{\parallel}^{\mathrm{A}}(x) = 2D_1(x)/(k + 1)^2 \tag{15a}$$

$$D_1(x) = 2(x - 1 + e^{-x})/x^2 \tag{15b}$$

Case A concerns scattering from the unstretched end of the polymer chain. The result $D_1(x)$ was obtained by Debye[12] for a random Gaussian coil. The factor 2 in eq 15a arises from the multiplicity of two chain ends.

$$S_{\parallel}^{\mathrm{B}}(x) = 2D_0(x)\exp[-q^2\langle Z_{1k}^2 \rangle/2]/(k + 1)^2 \tag{16a}$$

$$D_0(x) = (1 - e^{-x})/x \tag{16b}$$

The multiplicity is also twofold as indicated in Table I.

In case C, all monomer pairs are included in which one monomer is on a dangling end and the other on an internal submolecule. The result including multiplicity is

$$S_{\parallel}^{\mathrm{C}}(x) = 4D_0(x)J_0(x)\sum_{p=1}^{k-2}\exp[-q^2\langle Z_{1p}^2 \rangle/2]/(k + 1)^2 \tag{17a}$$

$$J_0(x) = \int_0^1\exp[-x(u - u^2) - u^2q^2\langle Z_{12}^2 \rangle/2]\,du \tag{17b}$$

The scattering in case D arises from monomer units on the same submolecule. The calculation is based on the same argument used for obtaining the scattering

$$S_{\parallel}^{\mathrm{D}}(x) = (k - 1)J_1(x)/(k + 1)^2 \tag{18a}$$

$$J_1(x) = 2\int_0^1\exp[-x(w - w^2) - w^2q^2\langle Z_{12}^2 \rangle/2](1 - w)\,dw \tag{18b}$$

Scattering from monomer pairs in which each monomer is in a separate submolecule within the network (not dangling ends) is given in case E by

$$S_{\parallel}^{\mathrm{E}}(x) = 2\sum_{p=1}^{k-3}(k - 2 - p)J_0^2(x)\exp[-q^2\langle Z_{p+1,q}^2 \rangle/2]/(k + 1)^2 \tag{19}$$

For a chain with many cross-links, $S_{\parallel}^{\mathrm{E}}(x)$ is the dominating term of $S_{\parallel}(x)$.

While the above calculations are specialized for $S_{\parallel}(x)$, generalization to other orientations or to isotropic swelling is simple. We return to this later when specific results are discussed.

As seen from eq 7–10, the mean square distances between segments is a linear function of the mean square distance between junctions. This latter is sensitive to network fluctuations, and the calculation of fluctuations needs special consideration. It will be shown that fluctuations in neighboring submolecules are strongly coupled.

Fluctuations of Cross-Link Junction Points. James[13] and James and Guth[14] showed in their analysis of the phantom network that the fluctuations of neighboring cross-links were large and that the mean squared fluctuation was half the mean squared junction-to-junction distance for a tetrafunctional network. This model was generalized by Graessley[15,16] and further developed by Flory,[17] who showed that for a network of functionality f, this may be written as

$$\langle \delta Z_{12}^2 \rangle = (2/f)\langle (Z_{12}^0)^2 \rangle \tag{20}$$

where $\langle (Z_{12}^0)^2 \rangle$ is the unperturbed mean squared displacement equal to $nb^2/3$. The superscript 0 refers throughout to distances in the undeformed network.

Consider the fluctuation of the individual junction points:

$$Z_{12} = Z_2 - Z_1 \tag{21a}$$

$$\delta Z_{12} = \delta Z_2 - \delta Z_1 \tag{21b}$$

$$\langle (\delta Z_{12})^2 \rangle = \langle (\delta Z_2)^2 \rangle - 2\langle \delta Z_1 \delta Z_2 \rangle + \langle \delta Z_1^2 \rangle \tag{21c}$$

All submolecules in this network contain the same number of segments n, and all junctions are of the same functionality f. Dangling ends are neglected here. It follows that $\langle (\delta Z_1)^2 \rangle = \langle (\delta Z_2)^2 \rangle$. The relationship between the fluctuations of junctions 1 and 2 is needed.

Consider the response of junction 2 to a virtual displacement δZ_1 of junction 1. Junction 2 is attached to $f - 1$ junctions other than junction 1, and its displacement may be written

$$\delta Z_2 = \delta Z_1/(f-1) + \epsilon \tag{22}$$

ϵ is a displacement arising from an instantaneous disequilibrium of forces to be expected of a system with Brownian motion. The first term, $\delta Z_1/(f-1)$, is the equilibrium displacement of junction 2. The important point is that ϵ is completely uncorrelated with δZ_1 or δZ_2. Substitution of eq 22 in eq 21c leads with eq 2 to

$$\langle \delta Z_1^2 \rangle = \frac{f-2}{f(f-1)}\langle (Z_{12}^0)^2 \rangle \tag{23}$$

This result has been reported by Flory,[18] presumably obtained by an argument similar to that given here.

Consider the quantity $\langle \delta Z_{1p}^2 \rangle$, where junctions 1 and p are separated by $p-2$ other junctions along an extended chain in a polymer network. These two junctions are only remotely connected by other topological paths through the network. It follows that

$$\langle \delta Z_{1p}^2 \rangle = \langle (\delta Z_1)^2 \rangle + \langle \delta Z_p^2 \rangle - 2\langle \delta Z_1 \delta Z_p \rangle = 2(\langle (\delta Z_1^2) \rangle - \langle (\delta Z_1 \delta Z_p) \rangle) \tag{24}$$

The number of junctions that are topological neighbors of order $p-1$ increases geometrically, and the displacement of each in response to the virtual displacement δZ decreases geometrically. Thus

$$\delta Z_p = \frac{\delta Z_1}{(f-1)^{p-1}} + \epsilon'(x) \tag{25}$$

Substitution of this result in eq 24

$$\langle (\delta Z_1 \delta Z_p) \rangle = \frac{\langle (\delta Z_1^2)^2 \rangle}{(f-1)^{p-1}} \tag{26a}$$

$$\langle \delta Z_{1p}^2 \rangle = \frac{2(f-2)}{f(f-1)}[1 - (f-1)^{1-p}]\langle (Z_{12}^0)^2 \rangle \tag{26b}$$

Note that for $p = 2$, the original result of eq 20 is recovered. To avoid trivial complications, it is assumed that dangling ends and other network defects may be ignored in the fluctuation computation.

Consider the evaluation of $\langle Z_{1p}^2 \rangle$

$$Z_{1p}^0 = \bar{Z}_{1p}^0 + \delta Z_{1p} \tag{27a}$$

$$\langle (Z_{1p}^0)^2 \rangle = \langle (\bar{Z}_{1p}^0)^2 \rangle + \langle \delta Z_{1p}^2 \rangle \tag{27b}$$

Since $\langle (Z_{1p}^0)^2 \rangle = (p-1)nb^2/3 = (p-1)\langle (Z_{12}^0)^2 \rangle$, eq 26b yields

$$\langle (\bar{Z}_{1p}^0)^2 \rangle = \left[p - 1 - \frac{2(f-2)}{f(f-1)}[1 - (f-1)^{1-p}] \right] \langle (Z_{12}^0)^2 \rangle \tag{28}$$

According to the phantom network model, the quantity $\bar{Z}$ deforms affinely and $\langle (\delta Z)^2 \rangle$ is independent of deformation. Therefore

$$\langle \bar{Z}_{1p}^2 \rangle = \lambda_z^2 \langle (\bar{Z}_{1p}^0)^2 \rangle \tag{29a}$$

$$\langle Z_{1p}^2 \rangle = \lambda_z^2 \langle (\bar{Z}_{1p}^0)^2 \rangle + \langle (\delta Z_{1p})^2 \rangle \tag{29b}$$

$$\langle Z_{1p}^2 \rangle = \left[\lambda_z^2 (p-1) - (\lambda_z^2 - 1)\frac{2(f-2)}{f(f-1)}(1 - (f-1)^{1-p}) \right] \langle (Z_{12}^0)^2 \rangle \tag{29c}$$

Note that for $p = 2$, eq 29 reduces to

$$\langle Z_{12}^2 \rangle = [\lambda_z^2 - (\lambda_z^2 - 1)(2/f)]\langle (Z_{12}^0)^2 \rangle \tag{30}$$

a result that figures prominently in the SANS calculations for end-linked elastomers. The result of eq 29 is used in the SANS calculation of $S_\parallel^B(x)$, $S_\parallel^C(x)$, and $S_\parallel^E(x)$ as required in eq 16a, 17a, and 19.

By combining eq 26b and 29, one may calculate the fluctuations between a pair of cross-links relative to the mean square distance. $\langle \delta Z_{1p}^2 \rangle$ is of the order of $^1/_3\langle (Z_{12}^0)^2 \rangle$ and increases only modestly as p varies from 2 to much higher values (eq 26b). However, $\langle Z_{1p}^2 \rangle$ is proportional to $p-1$, and the relative fluctuation $\langle \delta Z_{1p}^2 \rangle / \langle Z_{1p}^2 \rangle$ itself decreases as p^{-1}. To restate this, fluctuations of the junctions become less important as the junction points are separated by more submolecules. This is a result of the strong coupling of fluctuations of neighboring cross-links. It leads to important differences between the neutron scattering of end-linked and multiply-linked labeled chains.

It has been argued that junction fluctuations are sufficiently impeded by surrounding molecules that it is best to ignore them entirely. This is a view that is no longer generally accepted, but it is worthwhile to carry through the calculation with this assumption and to compare the results with experiments. The pertinent results are obtained from the equations for $\langle Z^2 \rangle$, eq 29 and 30, by letting the network functionality approach infinity. It is easy to understand why this is a natural result of the theory. The greater the functionality, the greater the elastic restoring force on a cross-link junction. Accordingly, the potential energy change associated with a virtual displacement increases with f, and the mean square magnitude of the fluctuation diminishes, approaching zero in the limit.

Junction fluctuations are certainly reduced by repulsive interactions of neighboring chain components in a real elastomer. An ingenious analysis of this effect has been presented by Flory.[18] In his view, fluctuations are present

but are smaller than that in a phantom network. He presents a persuasive argument that the fluctuations in a real network are anisotropic. It is implicit in his analysis that the effect of network entanglements on the forces in an elastomeric network can be largely understood in terms of impediments to junction fluctuations, a point of view currently considered as controversial. The Flory model has been included in an analysis of SANS of end-linked elastomeric networks elsewhere.[19,20] Its introduction into the theory of multiply-linked networks would not be difficult. This is not done, in part to avid further complicating the analysis and in part because fluctuations play only a lesser role in SANS calculations for multiply-linked elastomers.

Scattering Law and Radius of Gyration. The scattering law for a stretched elastomer measured parallel to the stretching direction takes the form

$$S_{\parallel}(x) = [2D_1(x) + 2D_0(x)Q_{k-1}(x) + 4D_0(x)J_0(x)R_k(x) + (k-1)J_1(x) + 2J_0^2(x)S_k(x)]/(k+1)^2 \quad (31a)$$

where $D_0(x)$, $D_1(x)$, $J_0(x)$, and $J_1(x)$ have been defined earlier,

$$Q_p(x) = \exp\left[-x\left(\lambda_z^2 p - (\lambda_z^2 - 1)\frac{2(f-2)}{f(f-1)}(1-(f-1)^{-p})\right)\right] \quad (31b)$$

$$R_k(x) = \sum_{p=0}^{k-2} Q_p(x) \quad (31c)$$

$$S_k(x) = \sum_{p=0}^{k-3} (k-2-p)Q_p(x) \quad (31d)$$

Equations 31a–d are found by substituting $\langle z_{ij}^2 \rangle$ for each of the categories in eq 14a. The equation for $S_{\perp}(x)$ is obtained from $S_{\parallel}(x)$ by replacing λ_z by λ_y.

If an elastomer is uniaxially stretched and if the volume does not change appreciably with elongation, the notation $\lambda_z = \lambda$ and $\lambda_x = \lambda_y = \lambda^{-1/2}$ becomes appropriate and will be adopted in the following calculations. The scattering law at an arbitrary angle cannot be obtained by a simple superposition of $S_{\parallel}(x)$ and $S_{\perp}(x)$. However, it is directly obtainable from a knowledge of $\langle z_{ij}^2 \rangle$ and $\langle y_{ij}^2 \rangle$ (see eq 12), which have been developed here in deriving $S_{\parallel}(x)$ and $S_{\perp}(x)$.

Equation 31a (with λ replacing λ_z) is also valid for chain deformation in swollen networks. Of course, the meaning of λ in a swelling experiment is the cube root of the volume ratio of the swollen to unswollen material, very different from λ, the uniaxial stretch ratio, in a deformation experiment.

In the special case where junctions do not fluctuate, the functions $R_k(x)$ and $S_k(x)$ are directly calculable. The results are

$$R_k(x) = \frac{1 - e^{-x\lambda_z^2(k-1)}}{1 - e^{-x\lambda_z^2}} \quad (32a)$$

$$S_k(x) = \frac{k - 2 - (k-1)e^{-x\lambda_z^2} + e^{-(k-1)x\lambda_z^2}}{(1 - e^{-x\lambda_z^2})^2} \quad (32b)$$

In a polymer network containing randomly distributed deuterated chains, the radius of gyration of a single chain is given by an expansion of the particle scattering function

$$S(x) = 1 - q^2 R_g^2/3 + \ldots \quad (33)$$

This is a result for an isotropic system. For an anisotropic sample, measurement at a particular azimuthal angle ϕ yields the projection of the radius of gyration along that direction. One may define R_ϕ^2 by

$$S_\phi(x) = 1 - q^2 R_\phi^2/3 + \ldots \quad (34a)$$

where the subscript ϕ refers to the azimuthal angle shown in Figure 2. Equation 34a when specialized to $\phi = 0$ becomes

$$S_{\parallel}(x) = 1 - q^2 R_{\parallel}^2/3 + \ldots \quad (34b)$$

and at $\phi = 90°$

$$S_{\perp}(x) = 1 - q^2 R_{\perp}^2/3 + \ldots \quad (34c)$$

The expansion of eq 31a in powers of x is achieved by straightforward calculation. Keeping linear terms in x only, one finds

$$S_{\parallel}(x) = 1 - \alpha_{\parallel} x = 1 - \alpha_{\parallel} n b^2 q^2/6 \quad (35)$$

where α is the sum of all the coefficients in the expansion of eq 31a. It follows that

$$R_{\parallel}^2 = \alpha_{\parallel} n b^2/2 \quad (36a)$$

Since $(R_g^0)^2$, the radius of gyration of the labeled molecule in the unstretched polymer, is $Nb^2/6$, where $N = n(k+1)$, $R_{\parallel}^2$ is given by

$$R_{\parallel}^2 = 3\alpha_{\parallel}(R_g^0)^2/(k+1) \quad (36b)$$

Similarly

$$R_{\perp}^2 = 3\alpha_{\perp}(R_g^0)^2/(k+1) \quad (36c)$$

Substituting the value of $\alpha_{\parallel}$ found from the expansion of eq 31a in eq 36b yields in the case of uniaxial stretching

$$R_{\parallel}^2/(R_g^0)^2 = 1 + (\lambda^2 - 1)[k^3 - k + (f-2)(4k+1) \times (k-1)/f - 6(T_1 + 2T_2 + T_3)]/(k+1)^3 \quad (37a)$$

$$\gamma_f = 2(f-1)/(f(f-2)) \quad (37b)$$

$$T_1 = \gamma_f[1 - (f-1)^{1-k}] \quad (37c)$$

$$T_2 = \gamma_f[(k-2) + (1-(f-1)^{2-k})/(f-2)] \quad (37d)$$

$$T_3 = \gamma_f[(k-2)(k-3)/2 + ((k-3)(f-1) - (k-2) + (f-1)^{3-k})/(f-2)^2] \quad (37e)$$

Equation 37a is adapted to the special case where cross-link junctions do not fluctuate by allowing f to become infinite. The result is

$$R_{\parallel}^2/(R_g^0)^2 = 1 + (\lambda^2 - 1)[(k-1)(2k^2 + 6k + 1)]/2(k+1)^3 \quad (38)$$

The expressions for $R_{\perp}^2$ are obtained by replacing λ^2 by λ^{-1} in eq 37a and 38. $R_g^2/(R_g^0)^2$ in a swelling experiment is given by the right side of eq 37a and 38 without change.

Numerical calculations of $R_{\parallel}^2$, $R_{\perp}^2$, $S_{\parallel}(x)$, and $S_{\perp}(x)$ are presented in the following section.

Numerical Results. Table II contains calculations of $R_{\parallel}/R_g^0$ and $R_{\perp}/R_g^0$ for labeled chains with multiple tetrafunctional cross-links. The quantity k is, as above, the number of cross-links per labeled chain. Results for end-linked chains are also listed for purposes of comparison. The formulas for end-linked chains are

$$R_{\parallel}^2 = [(R_g^0)^2/2][1 + \lambda^2 - (\lambda^2 - 1)(2/f)] \quad (39a)$$

(phantom network)

$$R_{\parallel}^2 = [(R_g^0)^2/2][1 + \lambda^2] \quad (39b)$$

(no junction fluctuations)

Equations for $R_{\perp}^2$ are based on the above, with λ^2 replaced by λ^{-1}. Some selected results are shown in Figure 3.

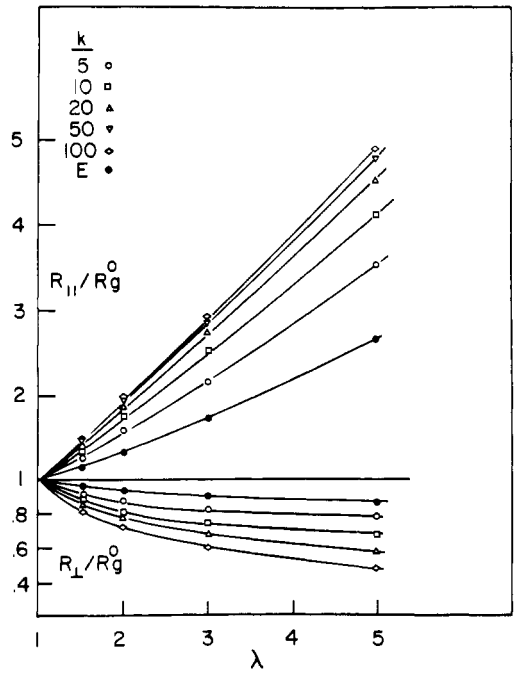

Figure 3. Ratios $R_{\parallel}/R_g^0$ and $R_{\perp}/R_g^0$ for a labeled chain containing multiple cross-links in a tetrafunctional phantom network. E symbolizes end-linked chains and k is the number of cross-links per chain.

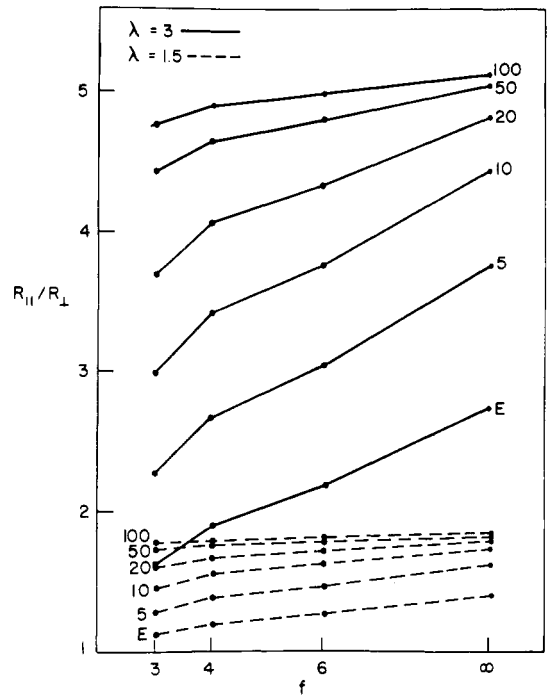

Figure 4. Dependence of $R_{\parallel}/R_{\perp}$ of multiply-cross-linked phantom networks on functionality is shown at two different elongations λ = 1.5 and λ = 3.0. Results are presented with the number of cross-links per chain varying from 5 to 100. E signifies end-linked chains.

$R_{\parallel}/R_{\perp}$ is a measure of molecular anisotropy in an anisotropically deformed rubber. Its dependence on cross-link junction functionality is shown in Figure 4 for multiply-linked and end-linked networks. At high k, $R_{\parallel}/R_{\perp}$ approaches the macroscopic anisotropy, $\lambda^{3/2}$. Also, the dependence on functionality decreases as k increases.

The principal differences between neutron scattering of end-linked chains and multiply-linked chains are displayed in the tables and figures. Stated briefly, the following results are seen.

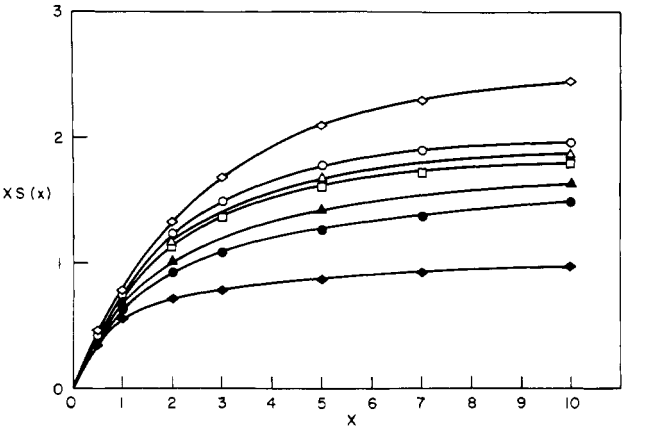

Figure 5. Kratky plots, $xS(x)$ vs. x are shown for anisotropically oriented tetrafunctional networks composed of end-linked chains and multiply-cross-linked chains at an elongation of λ = 1.5: (□) unperturbed, unstretched Gaussian chain; (△) end-linked chains, perpendicular orientation; (▲) end-linked chains, parallel orientation; (○) multiply-cross-linked chains, k = 5, perpendicular orientation; (●) multiply-cross-linked chains, k = 5, parallel orientation; (◇) multiply-cross-linked chains, k = 100, perpendicular orientation; (◆) multiply-cross-linked chains, k = 100, parallel orientation.

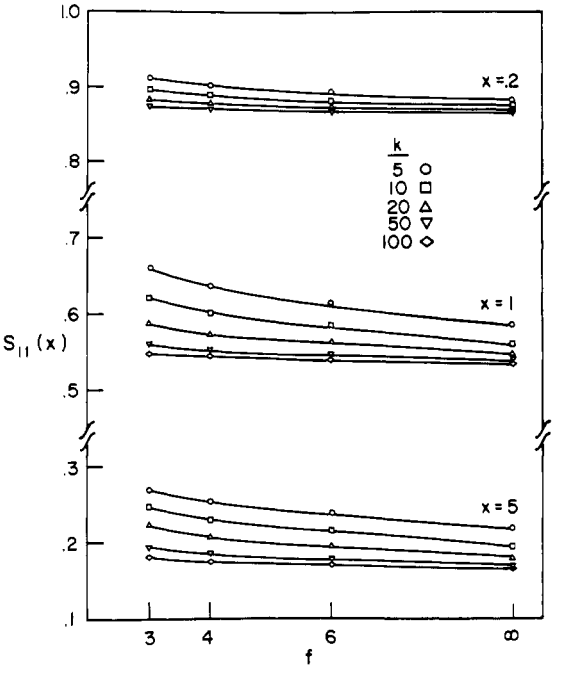

Figure 6. $S_{\parallel}(x)$ vs. functionality for multiply-cross-linked chains at three different values of x.

1. Multiply-linked chains deform to a greater extent than end-linked chains, and both the magnitude of the deformation and the anisotropy increase with increasing k.

2. Sensitivity to network functionality is much greater for end-linked chains.

3. The overall chain deformation for high k approaches the macroscopic deformation of the sample.

The radius of gyration and its projections along different directions reflect only the low-angle region of a SANS experiment. Further information is contained in the scattering function. Figure 5 contains plots of $xS(x)$ vs. x for end-linked chains and for multiply-linked chains with k = 5 and k = 100. Results are shown for a tetrafunctional network in both perpendicular and parallel projection.

In Figure 6, $S_{\parallel}(x)$ is shown at low, intermediate, and high x at different functionalities. The results at λ = 1.5 exhibit

Table II
$R_\parallel/R_g^0$ and $R_\perp/R_g^0$ for Tetrafunctional Multilinked Networks with Comparable Results on End-Linked Networks

	end-linked		multilinked				
λ	$f = 4$	fixed junctions	$k = 5$	$k = 10$	$k = 20$	$k = 50$	$k = 100$
			$R_\parallel/R_g^0$				
1.2	1.0536	1.105	1.101	1.139	1.166	1.185	1.192
1.5	1.1456	1.275	1.265	1.358	1.421	1.466	1.483
2.0	1.3229	1.581	1.563	1.740	1.856	1.939	1.969
3.0	1.7321	2.236	2.202	2.530	2.743	2.891	2.944
5.0	2.6458	3.666	3.542	4.148	4.535	4.804	4.900
8.0	4.093	5.701	5.595	6.599	7.237	7.678	7.836
			$R_\perp/R_g^0$				
1.2	0.9789	0.9574	0.9591	0.9420	0.9296	0.9202	0.9166
1.5	0.9574	0.9129	0.9163	0.8803	0.8533	0.8327	0.8249
2.0	0.9354	0.8660	0.8715	0.8138	0.7696	0.7349	0.7216
3.0	0.9129	0.8165	0.8242	0.7415	0.6756	0.6219	0.6007
5.0	0.8944	0.7746	0.7844	0.6780	0.5896	0.5140	0.4827
8.0	0.8839	0.7528	0.7610	0.6396	0.5353	0.4418	0.4014

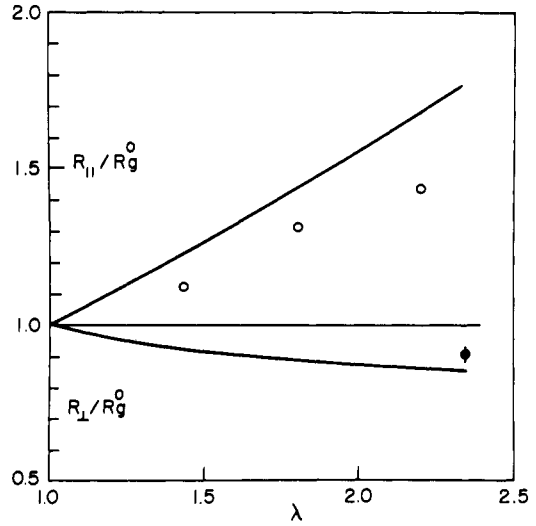

Figure 7. Phantom network calculation to compare with the experiments of Clough, Maconnachie, and Allen. Calculations are based on $f = 4$ and $k = 5$.

the insensitivity of $S_\parallel(x)$ to functionality at high k.

Comparison with Experiment. Clough et al.[5] measured $R_\parallel$ and $R_\perp$ of polystyrene networks containing 1.95% of D-tagged chains. These were cross-linked by γ radiation and the number of cross-links per labeled chain is approximately five. Their experiments with our calculations for tetrafunctional networks with five cross-links per chain are presented in Figure 7. It is clear that the calculated deformation for the multiply-linked phantom network is much greater than that experimentally observed. We have omitted a number of points obtained by Clough et al. for $R_\perp/R_g^0$ at low λ because the anisotropy is too small to justify further analysis.

The network deformation calculated for the fixed-junction case or for the Flory model of partially inhibited fluctuations is greater than that of a phantom network and clearly cannot be invoked to explain the lower anisotropy found in the SANS experiment. The idea that a network could unfold with little or no chain deformation upon swelling was implicit in the early SANS experiments of Benoit et al.[3] and elsewhere.[19-21] The driving force for achieving the necessary rearrangement of junction points is a lower elastic free energy when the chains are deformed to a lesser degree. This can be achieved without disturbing the homogeneous distribution of cross-links. It is limited by topological constraints imposed by the networks and by the volume occupied by the polymer chains themselves.

Table III
Network Unfolding Calculated from the Experiments of Clough et al. (Figure 7) and Eq 40

$R_\parallel/R_g^0$	$R_\perp/R_g^0$	λ	λ^*	α
1.12		1.432	1.22	0.53
1.32		1.80	1.56	0.36
1.42		2.20	1.80	0.42
	0.91	2.36	1.59	0.36[a]

[a] Calculated from $\lambda^{*-1} = \lambda^{-1}(1 - \alpha) + \alpha$, which is the analogue of eq 40 for perpendicular orientation.

SANS experiments on elastomers containing multiply-cross-linked labeled chains are particularly suitable for studying the affine hypothesis. Chain extension is, in principle, much greater for multiply-linked chains and therefore easier to measure. Secondly, junction fluctuations and their inhibition are of small importance to the multiply-linked case.

The network unfolding model is made concrete by defining a λ^*, which is an ensemble average of the deformation of junction pairs connected by a single submolecule in the network

$$\lambda^{*2} = \lambda^2(1 - \alpha) + \alpha \tag{40}$$

The phantom network corresponds to $\alpha = 0$. If $\alpha = 1$, the chain does not deform at all upon network stretching or swelling. λ^* is calculated from the data of Clough et al. by measuring chain deformation by SANS and setting λ^* as that value of λ calculated from the phantom network model. The results are shown in Table III.

Clough et al. compared their experiments with SANS calculations based on end-linked networks. They were not able to take into account the importance of multiple cross-links on a single labeled chain at that time, though they were aware of the need for a more suitable model.[22]

III. Discussion and Summary

The calculation of SANS results for the phantom network and fixed-junction model, previously carried out for end-linked chains, is extended to apply to labeled chains containing multiple cross-links. The latter shows much greater sensitivity to network deformation than do end-linked chains and much less sensitivity to network functionality. For this reason, SANS experiments on multiply-linked networks can exhibit junction rearrangement easily, since the influence of partially inhibited junction fluctuations plays a minor role.

If there are many cross-links per single labeled chain, the monomer units between cross-links are largely constrained. Accordingly, the radius of gyration and its

projections are largely determined by the position of the cross-links. This is evident in the anisotropy $R_{\parallel}/R_{\perp}$ at high k as shown in Figure 4.

The model chosen for calculation is simpler than a real randomly cross-linked network. All submolecules contain n segments, the number of cross-links per chain is constant, and the functionality of junction points adjoining chain ends is assumed to be the same as in the rest of the network. These assumptions are quite good if $k = 10$ or more. For small k, a random distribution of cross-link points will leave some molecules with 1 or 0 cross-links. These do not contribute to network elasticity nor are they deformed at equilibrium after stretching. This must be kept in mind if cross-links are introduced at random.

The direct relationship between polymer chain deformation and the theory of rubber elasticity makes SANS a unique tool for assessing the validity of several theoretical models. The theory also predicts swelling phenomena and elastic forces exerted by rubber in retraction. A comprehensive theory must account for these several phenomena, and ideally the different classes of experiment should be performed on identical samples. This is still an unfinished task.

References and Notes

(1) Benoit, H.; Cotton, J. P.; Decker, D.; Farnoux, B.; Higgins, J.; Jannink, G.; Ober, R.; Picot, C.; des Cloizeaux, J. *Macromolecules* **1974**, *7*, 863.
(2) Kirste, R. G.; Lehnen, B. R. *Makromol. Chem.* **1976**, *177*, 1137.
(3) Benoit, H.; Decker, D.; Duplessix, R.; Picot, C.; Rempp, P.; Cotton, J. P.; Farnoux, B.; Jannink, G.; Ober, R. *J. Polym. Sci., Polym. Phys. Ed.* **1976**, *14*, 2119.
(4) Hinkley, J. A.; Han, C. C.; Moser, B.; Yu, H. *Macromolecules* **1978**, *11*, 836.
(5) Clough, S. G.; Maconnachie, A.; Allen, G. *Macromolecules* **1980**, *13*, 774.
(6) Bastide, J.; Duplessix, R.; Picot, C. Colloque Franco-American Small Angle Scattering of X-Rays and Neutrons by Polymers, Sept 1980, lecture by C. Picot.
(7) Beltzung, M.; Herz, J.; Picot, C.; Bastide, J.; Duplessix, R. Abstracts of Communications, 27th International Symposium on Macromolecules, July 1981, Vol. 2, p 728.
(8) Han, C. C., private communication.
(9) Pearson, D. S. *Macromolecules* **1977**, *10*, 696.
(10) Warner, M.; Edwards, S. F. *J. Phys. A* **1978**, *11*, 1649.
(11) Ullman, R. *J. Chem. Phys.* **1979**, *71*, 436.
(12) Debye, P. Technical Report to Rubber Reserve, 1945. See also: *J. Phys. Colloid Chem.* **1947**, *51*, 18.
(13) James, H. M. *J. Chem. Phys.* **1947**, *15*, 651.
(14) James, H. M.; Guth, E. *J. Chem. Phys.* **1947**, *15*, 669.
(15) Graessley, W. W. *Macromolecules* **1975**, *8*, 186.
(16) Graessley, W. W. *Macromolecules* **1975**, *8*, 865.
(17) Flory, P. J. *Proc. R. Soc. London, Ser. A* **1976**, *351*, 351.
(18) Flory, P. J. *J. Chem. Phys.* **1977**, *66*, 5720.
(19) Ullman, R. *Macromolecules* **1982**, *15*, 582.
(20) Ullman, R. *ACS Symp. Ser.* **1982**, *No. 193*, Chapter XIII.
(21) Bastide, J.; Picot, C.; Candau, S. *J. Macromol. Sci., Phys.* **1981**, *B19*, 13.
(22) Allen, G., private communication.

Monomer Sequence Distributions in Ethylene–1-Hexene Copolymers

Eric T. Hsieh and James C. Randall*

Research and Development, Phillips Petroleum Company, Bartlesville, Oklahoma 74004.

Received February 24, 1982

ABSTRACT: A ^{13}C NMR method is presented for a quantitative determination of the respective comonomer distributions, the triad distributions, average sequence lengths, and run numbers in ethylene–1-hexene copolymers. Complete ^{13}C NMR chemical shift assignments were formulated after observation of two reference systems, a poly(1-hexene) and an ethylene–1-hexene copolymer containing only 1.9 mol % 1-hexene. A second copolymer having 17.3 mol % 1-hexene allowed an observation of all the intermediate connecting sequences between the extremes of the two reference systems. A subsequent quantitative procedure, which avoids errors from peak overlap and uncertainties in configurational assignments, was developed by using relative areas from well-spaced ^{13}C NMR spectral regions, defined uniquely in terms of contributing triad sequences. The method is designed to obtain a triad distribution with the highest possible accuracy, after which, structural information meaningful to the polymer chemist is extracted.

Introduction

Polyethylene density can be controlled through incorporation of a low amount of a 1-olefin, which maintains polymer chain linearity in an overall configurational sense but leads to short chain branches randomly spaced along the polymer backbone. The linear 1-olefins 1-butene, 1-hexene, and 1-octene are important commercially for this purpose and result in ethyl, butyl, and hexyl branches in the respective copolymers. It is interesting to establish just how these secondary comonomers are incorporated, that is, the extent to which they exist as isolated branches or as "clusters" such as 1,3-dialkyl branches, 1,3,5-trialkyl branches, and so forth. ^{13}C NMR is a useful technique for detecting comonomer sequencing; resonances from as many as five consecutive units have been uniquely detected in the ^{13}C NMR spectra of ethylene–propylene[1-3] and ethylene–1-butene[4,5] copolymers. We recently reported a ^{13}C NMR method[4] for measuring quantitatively the complete triad sequence distributions and subsequent run numbers, sequence lengths, and mole fractions in ethylene–1-butene copolymers and have now extended this method in principle and technique to a corresponding analysis of ethylene–1-hexene copolymers. The method is most dependent upon a set of correct assignments and an establishment of experimental conditions that lead to accurate measurements. A complete set of assignments, based on model copolymers, poly(1-hexene), and known polymer chemical shift behavior, is reported along with a discussion of the selection of discrete spectral regions that ensure an accurate quantitative analysis.

Experimental Section

The ^{13}C NMR spectra were recorded on a Varian XL-200 NMR spectrometer at 50.3 MHz. Instrument conditions were as follows: pulse anlge, 90°; pulse delay, 15 s; acquisition time, 1 s; spectral width, 8000 Hz; number of data points per spectrum, 16K and double-precision arithmetic employed during data acquisition.

0024-9297/82/2215-1402$01.25/0